Supporting Information

Klaus et al. 10.1073/pnas.1121236109

SI Materials and Methods

In Situ Hybridization and Histological Techniques. Control and mutant embryos were prepared in cold PBS, age-matched by their somite numbers, and fixed in 4% formaldehyde. Immunofluorescence and H&E staining were performed on 8-μm paraffin-embedded or 12-μm cryosections as described previously (1). The following primary antibodies were used: rabbit anti–β-galactosidase (Cappel); goat anti-GFP (Abcam); rabbit anti–phospho-Histon3 (Upstate); rabbit anti-Lef1 (Cell Signaling Technology); mouse anti–Nkx2-5 (Santa Cruz); and rabbit anti–phospho-Smad1/5/8 (Cell Signaling Technology). Mouse anti-Isl1/2 and mouse anti-troponinT2 (39.4D5 and CT3 monoclonal antibodies) were developed by T. Jessel and J. J.-C. Lin and were from the Developmental Studies Hybridoma Bank produced under the auspices of the Eunice Kennedy Shriver National Institute of Child Health and Development and maintained by the University of Iowa. Whole-mount in situ hybridization was performed using digoxygenin-labeled RNA probes (Roche) (1), followed by paraffin embedding and sectioning. The antisense transcripts of mouse cDNAs were as follow: Axin2 (NM_015732.3); Baf60c (NM_025891.3); Bmp2 (NM_007553.2); Bmp4-Ex4 (in situ probe has been generated to prime Exon4 flanked by LoxP sequences of the Bmp4 allele in conditional Bmp4 mice, X56848.1); Bmp7 (NM_007557.2); Gata4 (NM_008092.2); Hand2 (kindly provided by M. Blum, University of Hohenheim, Stuttgart-Hohenheim, Germany); Hey2 (NM_013904.1); Hey3 (NM_013905.3); Isl1 (NM_021459.2); LacZ (JN964117.1); Lef1 (NM_010703.3); Mef2c (BC026841.1);, Nkx2-5 (AF091351.1); PCDH7 (cloned from E9.25 cDNA, BC131967); Smad6 (AF010133.1); RBPJ (cloned from E9.25 cDNA, NM_001080927.1); Tbx20 (cloned from E9.25 cDNA, NM_020496.2); TNC (cloned from E9.25 cDNA, NM_011607.2); and Wnt2 (NM_023653.3).

Proliferation was assessed by immunofluorescence for phospho-Histone H3. Six heart sections from each of three to six E9.25 embryos of each genotype were used for quantification. Results are shown as means ± SEM, followed by students *t* test, with $P < 0.05$ considered as significant.

Microarray Data Analysis and Validation by Quantitative RT-PCR Analysis. Arrays were normalized using the BeadStudio Gene Expression Module v3.3.7 and quantile without background correction. Transcripts with low expression were removed by a minimum detection *P* value <0.05, and checking for outliers subsequently was performed using the principal component analysis with a correlation dispersion matrix and normalized eigenvector scaling. Differential expression was calculated using the Partek ANOVA statistics followed by a false discovery rate (FDR) multiple testing correction (2). Signal values of probe sets (ANOVA FDR < 0.05) were visualized by heatmap after normalization to a mean of 0 and an SD of 1.

For quantitative RT-PCR (qRT-PCR) analysis, total RNA of heart regions or FACS cells was extracted using TRIzol, RNase-free DNase treatment (Invitrogen), and phenol/chloroform extraction according to the manufacturer's instructions. First-strand cDNA was synthesized using 300 ng of total RNA and M-MLV reverse transcriptase (Promega) according to the manufacturer's instructions. qRT-PCR was performed in independent triplicates with an SYBR GreenER qPCR mix (Invitrogen), and relative mRNA expression was normalized to *GAPDH* (primer sets are available from A.K. upon request).

Cell Culturing. Sorted cells, 0.2×10^4 to 0.35×10^5, were seeded onto individual wells of a 96-well plate, coated with 3% (wt/vol) agarose, in 12.5% (vol/vol) Matrigel (BD Biosciences) in Cor.AT medium (AxioGenesis), supplemented with hBmp4 (3.12 ng/mL) (Biosource) and hActivin A (16 ng/mL) (Invitrogen) (3). Cultures were supplemented every 48 h with hBmp4 and hActivin A. Seven days later cultures were harvested, cytospun, fixed, and analyzed by fluorescence microscopy.

1. Huelsken J, et al. (2000) Requirement for beta-catenin in anterior-posterior axis formation in mice. *J Cell Biol* 148:567–578.
2. Benjamini Y, Hochberg Y (1995) Controlling the false discovery rate: A practical and powerful approach to multiple testing. *J R Stat Soc, B* 57:289–300.
3. Kattman SJ, et al. (2011) Stage-specific optimization of activin/nodal and BMP signaling promotes cardiac differentiation of mouse and human pluripotent stem cell lines. *Cell Stem Cell* 8:228–240.

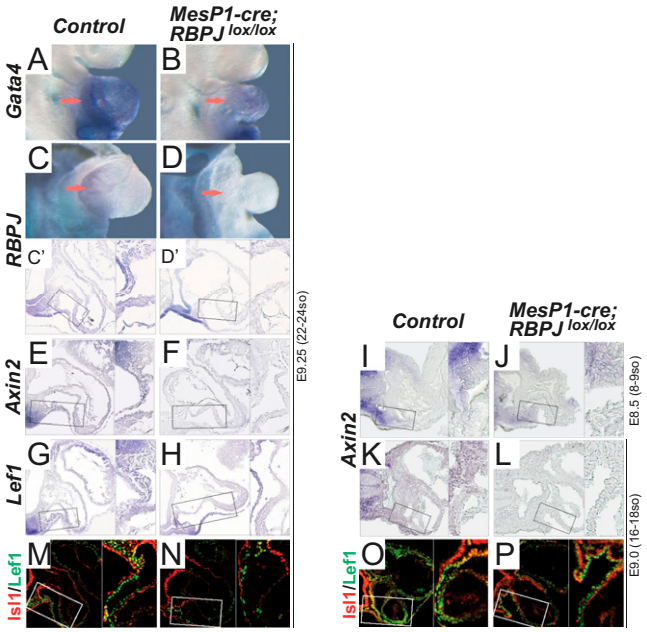

Fig. S1. Regulation of Wnt target genes in *RBPJ* mutant embryos. (*A–L*) Lateral views of whole-mount in situ hybridizations and of sections stained for *Gata4*, *RBPJ*, *Axin2*, and *Lef1* in controls and *RBPJ* single mutants (arrows mark right ventricles) at E8.5, E9.0, and E9.25. Note that RBPJ expression is lost in mutants in the splanchnic mesoderm, myocardium, and endocardium (see magnifications in *C′* and *D′*) where the expression of *Axin2* and *Lef1* is reduced markedly (magnifications at right in *E–L*). (*M–P*) Immunofluorescence analysis of Isl1 (red) and Lef1 (green) shows fewer cells with colocalization in the splanchnic mesoderm of *RBPJ* mutant embryos (see magnifications at right) at E9.0 and E9.25.

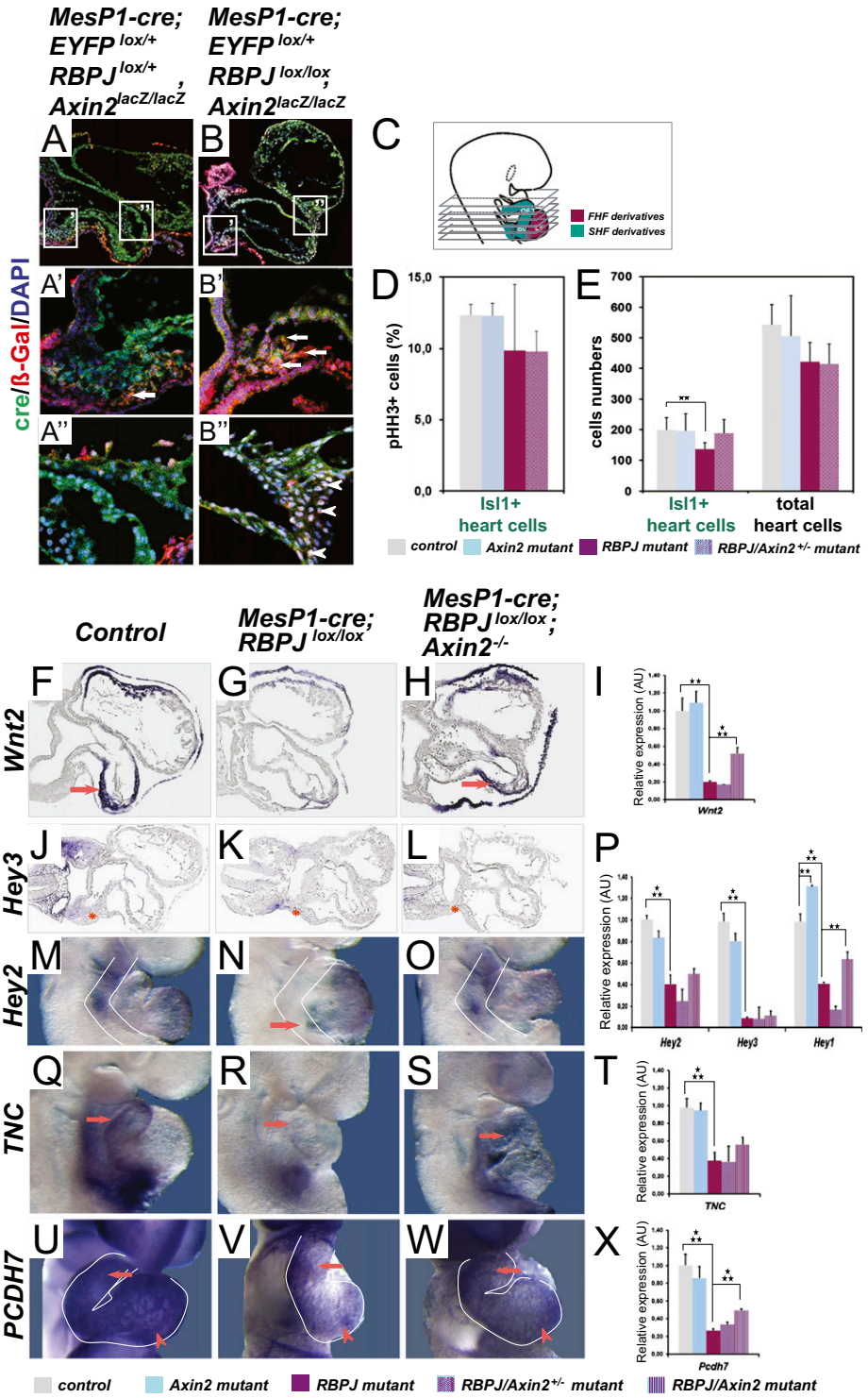

Fig. S2. *RBPJ*/*Notch* cross talks with *Wnt*/*β-catenin* signaling in the heart at E9.25. (*A–B″*) Immunofluorescence analysis of β-galactosidase (red) and cre (GFP, green) shows increased level of β-galactosidase in the splanchnic mesoderm (marked by arrows in magnifications of *A′* and *B′*) and ventricular walls (marked by arrowheads in *B″*) of *RBPJ*/*Axin2* double-mutant vs. *Axin2* single-mutant hearts. (*C*) Scheme indicates FHF (red) and SHF (green) derivatives in six transverse sections of mouse embryos at E9.25 that were used for quantification. (*D*) Quantification of proliferation as assessed by percentage of pHH3$^+$ nuclei in Isl1$^+$ cells in controls (gray bars), *RBPJ* single mutants (magenta bars), *Axin2* single mutants (blue bars), and *RBPJ*/*Axin2*$^{+/-}$ double mutants (stippled bars). (*E*) Average number of Isl$^+$ cells and total number of cells per section at E9.25. Note that the number of Isl1-expressing cells is significantly reduced in *RBPJ* single mutants (137 ±20.6, $P = 0.0065$) and that loss of one allele of *Axin2* is sufficient to normalize the numbers of Isl$^+$ cells in *RBPJ*/*Axin2*$^{+/-}$ double mutants (189 ±43.8, $P = 0.744$). Error bars represent SEM ($n = 3–6$). $^{**}P < 0.01$. (*F–X*) Lateral and frontal views of whole-mount in situ hybridizations of embryos. and of sections thereof, for *Wnt2*, *Hey3*, *Hey2*, *TNC*, and *PCDH7* (outflow tracts and right ventricle are marked by arrows, left ventricle by arrowheads, splanchnic mesoderm by asterisk in *J–L*, and SHF by lines) and corresponding qRT-PCR quantifications in controls, *RBPJ* single mutants, *RBPJ*/*Axin2*$^{+/-}$, *RBPJ*/*Axin2* double mutants, and *Axin2* single mutants. Error bars represent SEM ($n = 4$). $^{**}P < 0.01$, $^{***}P < 0.005$. AU, arbitrary units.

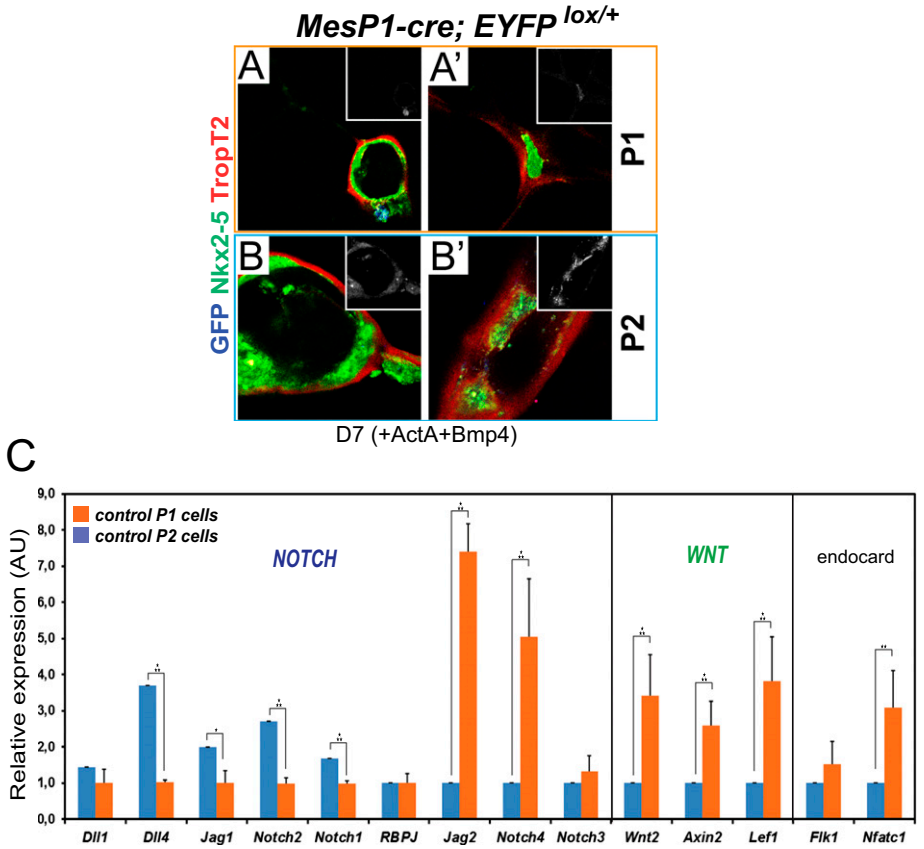

Fig. S3. Characterization of P1 and P2 cells after enrichment by FACS. (*A*–*B'*) Immunofluorescence analysis of GFP (blue, and in *Insets*), Nkx2-5 (green), and TropT2 (red) shows that P1 cells differentiate into TropT2-expressing cardiomyocytes after 7d of culture in the presence of Activin A and Bmp4. (*C*) qRT-PCR analysis of mRNA expression in P1 cells (orange) and P2 cells (blue) of controls shows higher expression of Wnt/β-catenin pathway components and target genes in cardiac progenitor populations. Error bars represent SEM ($n = 5$). $^{*}P < 0.05$, $^{**}P < 0.01$, $^{***}P < 0.001$. AU, arbitrary units.

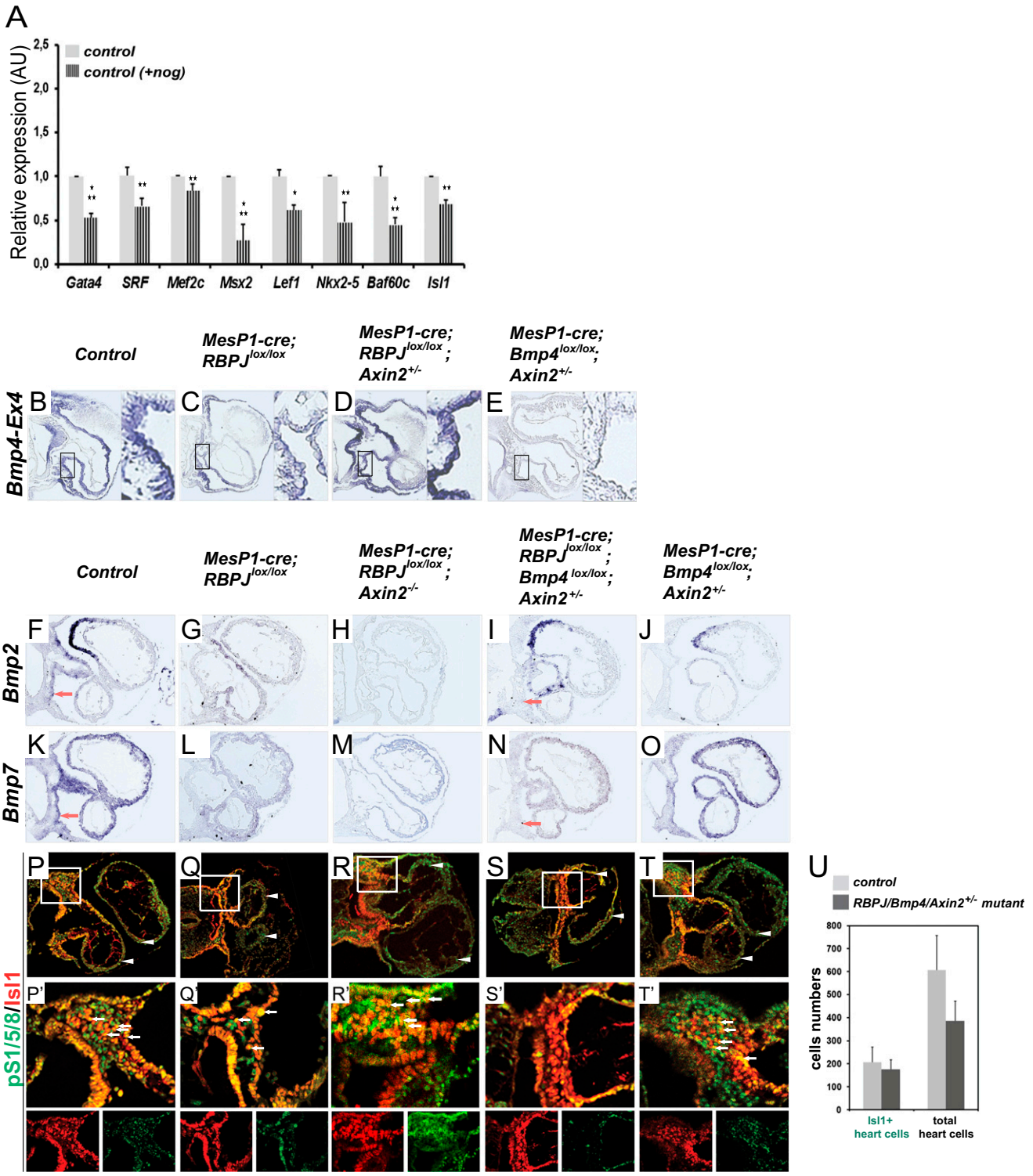

Fig. S4. The *Bmp4* mutation suppresses Bmp signaling in the anterior SHF of *RBPJ/Axin2* mutants at E9.25. (*A*) Effect of Noggin treatment on embryo cultures at E8.75–9.25. qRT-PCR analysis of mRNA expression levels of the indicated genes of controls in the absence (gray bars) or presence of Noggin (+Noggin; striped bars). Error bars represent SEM ($n = 6$). (*B–E*) In situ hybridizations on transverse sections for *Bmp4-Ex4* in controls, *RBPJ* single mutants, *RBPJ/Axin2*$^{+/-}$ mutants, and *Bmp4/Axin2*$^{+/-}$ mutants show that *Bmp4* has been ablated in Bmp4/Axin2$^{+/-}$ mutants, *Bmp4* expression is reduced in *RBPJ* single mutants, and *Bmp4* is restored in *RBPJ/Axin2*$^{+/-}$ mutants. The *Bmp4-Ex4* in situ probe has been generated to prime Exon4 flanked by LoxP sequences of the targeted *Bmp4* allele in conditional *Bmp4* mice. Compare magnifications of the anterior SHF at the right in *C*, *D*, and *E*. (*F–O*) In situ hybridization on transverse section for *Bmp2* and *Bmp7* in control, *RBPJ* single-mutant, RBPJ/Axin2 double-mutant, *RBPJ/Bmp4/Axin2*$^{+/-}$ triple-mutant, and *Bmp4/Axin2*$^{+/-}$mutant embryos. The expression of *Bmp2* and *Bmp7* is lost in the splanchnic mesoderm (marked by arrows) of triple mutants. (*P–T'*) Immunofluorescence analysis of Isl1 (red) and pSmad1/5/8 (green) in control, *RBPJ* single-mutant, *RBPJ/Axin2* double-mutant, *RBPJ/Bmp4/Axin2*$^{+/-}$ triple-mutant, and *Bmp4/Axin2*$^{+/-}$ mutant embryos (magnifications are shown in *P'–T'*; with single-channel images of magnifications shown below each panel). pSmad1/5/8 and Isl1 coexpression in the splanchnic mesoderm is marked by arrows, and pSmad1/5/8^{+} cells in the ventricular walls are marked by arrowheads. (*U*) Average numbers of Isl^{+} cells and total cell numbers per section in controls (light gray bars) and *RBPJ/Bmp4/Axin2*$^{+/-}$ triple mutants (dark gray bars). Note that the number of Isl^{+} cells is unaltered in *RBPJ/Bmp4/Axin2*$^{+/-}$ triple mutants (175.28 ±42.2, $P = 0.47$). Error bars represent SEM ($n = 3$).

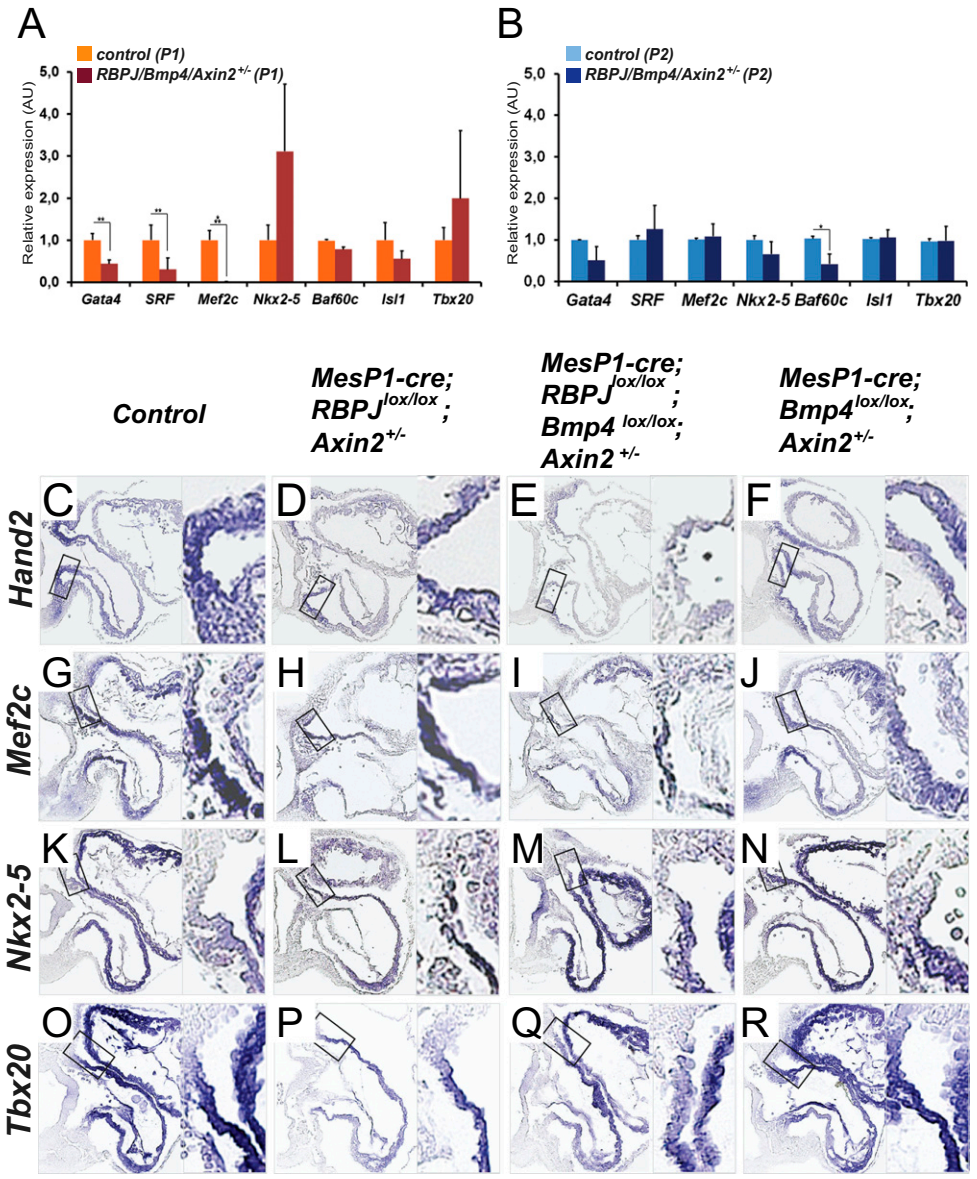

Fig. S5. Wnt/β-catenin and Bmp signaling downstream of Notch/RBPJ target different sets of cardiac-specific transcription factors. (*A* and *B*) qRT-PCR analysis of mRNA expression in the cardiac progenitor population (P1) (*A*) and in P2 (*B*) of controls (*MesP1-cre;EYFP*$^{lox/+}$; *Bmp4*$^{lox/+}$;*RBPJ*$^{lox/+}$;*Axin2*$^{+/-}$; light bars) and triple mutants (*MesP1-cre;EYFP*$^{lox/+}$; *RBPJ*$^{lox/lox}$;*Bmp4*$^{lox/lox}$;*Axin2*$^{+/-}$, dark bars). Error bars represent SEM ($n = 4$). *$P < 0.05$, **$P < 0.01$, ***$P < 0.005$. AU, arbitrary units. (*C–R*) In situ hybridization on transverse sections for *Hand2*, *Mef2c*, *Nkx2-5*, and *Tbx20* in control, *RBPJ/Axin2*$^{+/-}$, *RBPJ/Bmp4/Axin2*$^{+/-}$ triple-mutant, and *Bmp4/Axin2*$^{+/-}$ mutant embryos. The region of SHF cells is outlined and is magnified at the right.

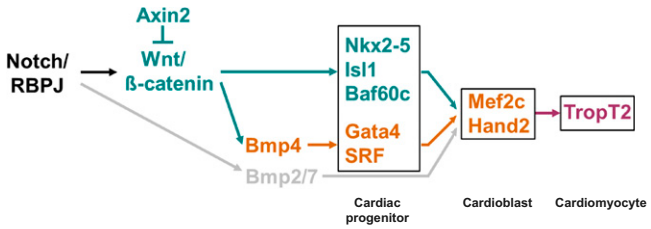

Fig. S6. Model depicting the sequential regulation of cardiac-specific transcription factors by Notch, canonical Wnt, and Bmp signaling in the differentiation of cardiac progenitors in the anterior SHF. Wnt/β-catenin is an irreversible downstream effector of Notch signaling controlling the expression of essential transcription factors in cardiac progenitors, either directly, via *Baf60c*, *Nkx2-5*, and *Isl1*, or indirectly, via Bmp4 signaling, which targets *Gata4* and *SRF*. The cooperation of Wnt/β-catenin and Bmp signals then induces further factors essential for cardioblast formation and differentiation, such as *Mef2c*, *Hand2,* and *TropT2*. *Bmp2* and *Bmp7* are not controlled by Wnt signaling.

Other Supporting Information Files

Table S1 (DOC)
Table S2 (DOC)
Table S3 (DOC)